CONDITIONAL MEAN RISK SHARING IN THE INDIVIDUAL MODEL WITH GRAPHICAL DEPENDENCIES

Michel Denuit, Christian Y. Robert

REPRINT | 2022 / 20

UCLouvain
LIDAM
ISBA | Louvain Institute of Data Analysis and Modeling in economics and statistics

ISBA
Voie du Roman Pays 20 - L1.04.01
B-1348 Louvain-la-Neuve
Email : lidam-library@uclouvain.be
https://uclouvain.be/en/research-institutes/lidam/isba/publication.html

CONDITIONAL MEAN RISK SHARING FOR DEPENDENT RISKS USING GRAPHICAL MODELS

Michel Denuit
Institute of Statistics, Biostatistics and Actuarial Science - ISBA
Louvain Institute of Data Analysis and Modeling - LIDAM
UCLouvain
Louvain-la-Neuve, Belgium
michel.denuit@uclouvain.be

Christian Y. Robert
Laboratory in Finance and Insurance - LFA
CREST - Center for Research in Economics and Statistics
ENSAE
Paris, France
chrobert@ensae.fr

August 25, 2020

Abstract

Conditional mean risk sharing appears to be effective in collaborative insurance to distribute total losses among participants. This paper develops analytical results for this risk sharing rule when risks are zero-augmented random variables whose joint occurrences distributions and claim amount distributions are based on network structures and may be characterized by graphical models. More specifically we consider the Ising model for occurrences and decomposable graphical models for the claim amount structures. Such models are typically useful for modeling operational risk or cyber security risk.

Keywords: Graphical models, Ising model, decomposable graphs, size-biased transform.

JEL Classification: G22

1 Introduction

Graphical models are a very useful tool to factorize probability distributions over a multi-dimensional space. They use graph-based representations to express e.g. the conditional dependence structure within the random variables or to characterize groups of random variables as common factors. They are commonly used in Bayesian statistics and machine learning. Their popularity has grown in recent years due to the development of efficient algorithms for performing computationally intensive inference in high-dimensional models. They have been widely used in applications ranging from causal inference, information extraction to speech recognition, natural language processing and computer vision. Recently Ramsahai (2020) showed that some actuarial models in current practice can be expressed graphically to exploit the advantages of such an approach and concluded that the graphical models can be very useful for applications e.g. in the modelling of home insurance property damage. Oberoi et al. (2020) applied statistical graphical models to simulate economic variables for the purpose of risk calculations over long time horizons. Lin et al. (2014) also considered Bayesian networks (which are a particular case of graphical models) to perform convolution of loss distributions required to aggregate risk in the presence of common causal dependencies.

This paper aims at contributing to the literature on risk sharing when risks are dependent and their distributions can be efficiently summarize with graphical models. Denuit (2019, 2020b) demonstrated that conditional mean risk sharing introduced by Denuit and Dhaene (2012) is an effective mechanism in collaborative insurance to distribute total losses among participants. Denuit and Robert (2020a,b,c) established several attractive properties of this sharing rule. In particular they showed that the conditional expectation defining the conditional mean risk sharing is in general asymptotically increasing in the total loss under mild technical assumptions, which ensures that the risk exchange is Pareto-optimal and that all participants have an interest to keep total losses as small as possible. Recently Denuit and Robert (2020d) developed analytical formulas of the conditional mean risk sharing rule for general risk multivariate distributions (without assuming independence between risks). They proved that the conditional expectations can be expressed from the size-biased version of the vector of risks. Several examples are discussed, including Liouville and infinitely divisible multivariate distributions, for which the conditional expectations are linear in the total loss amount. In general analytical expressions of the multivariate distributions of the size-biased transform are difficult to derive from the original multivariate distributions of the vectors of risks.

In this paper, we assume that the risks can be represented by zero-augmented random variables whose joint occurrences distributions and claim amount distributions are based on network structures and may be derived from graphical models. More specifically we assume that joint occurrences may be characterized by the famous Ising model, named after the physicist Ernst Ising. The claim amount structures will be supposed to be based on decomposable graphical models for which it is known that junction trees can be used to obtain an explicit form for the factorization of the multivariate distributions of individual claim amounts.

Such models are typically useful for modeling operational risk or cyber security risk. Operational risk management needs quantitative risk models to constitute a sound basis for fruitful discussions on the acceptance or the mitigation of such specific risks. Detailed causal modelling at business process level is required for the understanding of organization specific input, highlight the criticality of causal factors, identify the potential lack of controls/barriers, etc. Such an approach may create more value than a risk model based solely on actuarial techniques (see e.g. Politou and Giudici (2009)). Cyber risks refer to threats to businesses or individuals such as data breaches or malicious cyber hacks on work computer systems. One property that distinguishes cyber risks from conventional risk is the network environment. IT-related resources controlled by a firm include physical resources associated such as IT infrastructure, databases, networks and software packages, as well as non-physical (human) resources such as organization-wide IT expertise and IT managers' skills. IT resources are strongly interconnected inside the firm, but also between firms by the internet network. Cyber risks emerge from this interconnection, therefore the analysis of risk and potential losses may fruitfully take into account the inter-dependencies between connected nodes of the network through graphical models (see e.g. Xie et al. (2010)).

The remainder of this paper is organized as follows. In Section 2, we first recall the definitions of the conditional mean risk sharing rule and of the size-biased versions of multivariate distributions. Then, we establish useful representations of the individual contributions to the pool under conditional mean risk sharing rule in the case of multivariate zero-augmented vector of risks. Section 3 is devoted to the presentation of the Ising model and provides a result on the characterization of their size-biased versions. Section 4 presents the theory of decomposable graphical models for absolutely continuous multivariate distributions and explains how to derive their size-biased versions. The results are applied in Section 5 where an extensive numerical illustration shows the flexibility of graphical models. The final Section 6 briefly discusses the results. An appendix provides the specifications of the graphical models considered in Section 5 (number of vertices, number of edges, sets of maximal cliques, sets of minimal seperators, precision matrices of the associated multivariate Gaussian random variables, etc.).

2 Conditional mean sharing rule for dependent zero-augmented risks

We consider n participants to an insurance pool, numbered $i \in \{1, 2, \ldots, n\}$. Participant i faces a zero-augmented risk X_i, i.e. X_i is a positive random variable with a strictly positive probability equal to zero, $\mathrm{P}[X_i = 0] > 0$, and absolutely continuous otherwise. We write $X_i = I_i C_i$ where I_i is a Bernoulli random variable and C_i is a strictly positive absolutely continuous random variable modeling the claim amount. We assume that these claim amounts C_i are independent and independent on the vector $\mathbf{I} = (I_1, ..., I_n)$ of possibly correlated Bernoulli random variables (see Dai et al. (2013)). We denote by $S = \sum_{i=1}^n X_i$ the sum of the risks.

In the design of a risk sharing scheme, it is important that the sharing rule between participants represented by the functions h_i, $i \in \{1, 2, \ldots, n\}$, is both intuitively acceptable and transparent. In that respect, the conditional mean risk sharing (or allocation) h_i^* proposed by Denuit and Dhaene (2012) is particularly attractive and is defined as

$$h_i^*(S) = \mathrm{E}[X_i|S], \;\; i = 1, 2, \dots, n. \tag{2.1}$$

In words, participant i must contribute the expected value of the risk X_i brought to the pool, given the total loss S. Clearly, the conditional mean risk sharing (2.1) allocates the full risk S as we obviously have

$$\sum_{i=1}^{n} h_i^*(S) = \sum_{i=1}^{n} \mathrm{E}[X_i|S] = S$$

so that the sum of participants' contributions covers the entire loss S. In the expected utility setting, every risk-averse decision-maker prefers $h_i^*(S)$ over the initial risk X_i so that the conditional mean risk sharing rule appears to be beneficial to all participants (as an application of Jensen's inequality).

Denuit and Robert (2020d) developed analytical formulas of the conditional mean risk sharing rule for general risk multivariate distributions (without assuming independence between risks). They are based on the size-biased version of the vector of risks. For each $i \in \{1, 2, \dots, n\}$, we define the i-th size-biased version of $\boldsymbol{X}$ by the random vector $\boldsymbol{X}^{[i]} = (X_1^{[i]}, \dots, X_n^{[i]})$ with joint distribution function $F_{\boldsymbol{X}^{[i]}}$ given by

$$\begin{aligned} F_{\boldsymbol{X}^{[i]}}(x_1, \dots, x_n) &= \int_0^{x_1} \cdots \int_0^{x_n} \frac{y_i \mathrm{d}F_{\boldsymbol{X}}(y_1, \dots, y_n)}{\mathrm{E}[X_i]} \\ &= \frac{\mathrm{E}[X_i|X_1 \leq x_1, \dots, X_n \leq x_n]}{\mathrm{E}[X_i]} F_{\boldsymbol{X}}(x_1, \dots, x_n). \end{aligned} \tag{2.2}$$

Distribution (2.2) has been considered by Arratia et al. (2019) in relation to size-biasing sums of random variables. The distribution function (2.2) is a multivariate weighted version of the distribution function for $\boldsymbol{X}$. Multivariate weighted distributions have been reviewed by Navarro et al. (2006). The weight function w corresponding to (2.2) is $w(x_1, \dots, x_n) = x_i/\mathrm{E}[X_i]$ that has been considered in Jain and Nanda (1995). It is proved in Proposition 3.1 iii) of Denuit and Robert (2020d) that, if $X_1, \dots, X_n$ are zero-augmented random variables with positive probability masses at the origin and probability density functions over $(0, \infty)$ then $\mathrm{E}[X_i|S = 0] = 0$ and, for any $s > 0$, the representation

$$\mathrm{E}[X_i|S = s] = \frac{\mathrm{E}\left[X_i\right] f_{X_1^{[i]}+\ldots+X_n^{[i]}}(s)}{\sum_{j=1}^{n} \mathrm{E}\left[X_j\right] f_{X_1^{[j]}+\ldots+X_n^{[j]}}(s)}$$

holds true.

In the particular case of our model described above, we can say more on the distribution of $\boldsymbol{X}^{[i]}$ for $i \in \{1, 2, \dots, n\}$. Let us recall that the size-biased version $\tilde{X}$ of a positive (univariate) random variable X is defined through its distribution function by

$$\mathrm{P}[\widetilde{X} \leq t] = \frac{1}{\mathrm{E}[X]} \int_0^t x \mathrm{d}F_X(x).$$

The distribution of $\boldsymbol{X}^{[i]}$, where $X_i = I_i C_i$ $i \in \{1, 2, \dots, n\}$, has the following representation.

Proposition 2.1. *We have*

$$\boldsymbol{X}^{[i]} \stackrel{\mathrm{d}}{=} \left(I_1^{[i]}C_1, ..., I_{i-1}^{[i]}C_{i-1}, \tilde{C}_i, I_{i+1}^{[i]}C_{i+1}, ..., I_n^{[i]}C_n\right),$$

where $\boldsymbol{I}^{[i]}, C_1, ..., C_{i-1}, \tilde{C}_i, C_{i+1}, ..., C_n$ *are all independent, and* $\boldsymbol{I}^{[i]} \stackrel{\mathrm{d}}{=} \boldsymbol{I}|I_i = 1$.

Proof. We have

$$\begin{aligned}
F_{\boldsymbol{X}^{[i]}}(x_1, \ldots, x_n) &= \frac{1}{\mathrm{E}\left[X_i\right]}\mathrm{E}\left[X_i \mathrm{I}[X_1 \leq x_1, ..., X_n \leq x_n]\right] \\
&= \frac{1}{\mathrm{E}\left[I_iC_i\right]}\mathrm{E}\left[I_iC_i \mathrm{I}[I_1C_1 \leq x_1, ..., I_nC_n \leq x_n]\right] \\
&= \frac{1}{\mathrm{E}\left[I_iC_i\right]}\mathrm{E}\left[\mathrm{E}\left[I_iC_i \mathrm{I}[I_1C_1 \leq x_1, ..., I_nC_n \leq x_n]|I_1, ..., I_n\right]\right].
\end{aligned}$$

But note that

$$\begin{aligned}
& \mathrm{E}\left[I_iC_i \mathrm{I}[I_1C_1 \leq x_1, ..., I_nC_n \leq x_n]|I_1, ..., I_n\right] \\
= \; & \mathrm{E}\left[I_iC_i \mathrm{I}[I_iC_i \leq x_i|I_1, ..., I_n\right] \prod_{j \neq i} \mathrm{P}\left[I_jC_j \leq x_j|I_1, ..., I_n\right]
\end{aligned}$$

and

$$\begin{aligned}
& \frac{\mathrm{E}\left[I_iC_i \mathrm{I}[I_iC_i \leq x_i]|I_1, ..., I_n\right]}{\mathrm{E}\left[I_iC_i\right]} \\
= \; & \frac{\mathrm{E}\left[I_iC_i \mathrm{I}[I_iC_i \leq x_i]|I_1, ..., I_n\right]}{\mathrm{E}\left[I_iC_i|I_1, ..., I_n\right]} \times \frac{\mathrm{E}\left[I_iC_i|I_1, ..., I_n\right]}{\mathrm{E}\left[I_iC_i\right]} \\
= \; & \frac{\mathrm{E}\left[I_iC_i \mathrm{I}[I_iC_i \leq x_i]|I_1, ..., I_n\right]}{\mathrm{E}\left[I_iC_i|I_1, ..., I_n\right]} \times \frac{I_i}{\mathrm{E}\left[I_i\right]}
\end{aligned}$$

and therefore

$$F_{\boldsymbol{X}^{[i]}}(x_1, \ldots, x_n) = \mathrm{E}\left[\frac{\mathrm{E}\left[I_iC_i \mathrm{I}[I_iC_i \leq x_i]|I_1, ..., I_n\right]}{\mathrm{E}\left[I_iC_i|I_1, ..., I_n\right]} \times \frac{I_i}{\mathrm{E}\left[I_i\right]} \prod_{j \neq i} \mathrm{P}\left[I_jC_j \leq x_j|I_1, ..., I_n\right]\right].$$

We deduce that $\boldsymbol{X}^{[i]} \stackrel{\mathrm{d}}{=} \left(I_1^{[i]}C_1, ..., I_{i-1}^{[i]}C_{i-1}, \tilde{C}_i, I_{i+1}^{[i]}C_{i+1}, ..., I_n^{[i]}C_n\right)$.

Moreover, for $\mathbf{x} \in \{0, 1\}^n$,

$$\mathrm{P}[\boldsymbol{I}^{[i]} = \mathbf{x}] = \frac{1}{\mathrm{E}[I_i]}\mathrm{P}[\boldsymbol{I} = \mathbf{x}]1[x_i = 1] = \mathrm{P}[\boldsymbol{I} = \mathbf{x}|I_i = 1].$$

□

Since the claim amount of participant i may be the result of an aggregation of several individual claims in practice, we will moreover assume that the absolutely continuous part of X_i may be written as a sum: $C_i = \sum_{j=1}^{n_i} Z_{ij}$ where $\mathbf{Z}_i = (Z_{i1}, ..., Z_{in_i})$ is a vector of non-negative random variables of size $n_i \in \{1, 2, \ldots\}$. The size-biased version of C_i may be characterized in the following way. Define the random variable K_i valued in $\{1, 2, \ldots, n_i\}$, independent of $\mathbf{Z}_i$ and of $\boldsymbol{Z}_i^{[1]}, \ldots, \boldsymbol{Z}_i^{[n_i]}$ such that $\mathrm{P}[K_i = k] = \frac{\mathrm{E}[Z_{ik}]}{\mathrm{E}[C_i]}$ for $k \in \{1, 2, \ldots, n_i\}$. The following proposition is derived from Section 2.4 in Denuit and Robert (2020d).

Proposition 2.2. *We have*

$$\tilde{C}_i \stackrel{\mathrm{d}}{=} \sum_{j=1}^{n_i} Z_{ij}^{[K]} = \begin{cases} Z_{i1}^{[1]} + \ldots + Z_{in_i}^{[1]} \text{ with probability } \frac{\mathrm{E}[Z_{i1}]}{\mathrm{E}[C_i]} \\ Z_{i1}^{[2]} + \ldots + Z_{in_i}^{[2]} \text{ with probability } \frac{\mathrm{E}[Z_{i2}]}{\mathrm{E}[C_i]} \\ \vdots \\ Z_{i1}^{[n_i]} + \ldots + Z_{in_i}^{[n_i]} \text{ with probability } \frac{\mathrm{E}[Z_{in_i}]}{\mathrm{E}[C_i]} \end{cases}.$$

In the next sections, we present the graphical models used for $\boldsymbol{I}$ and $\mathbf{Z}_i$, $i \in \{1, 2, \ldots, n\}$.

3 Ising model

The Ising model is a classical example of a graphical model for binary random variables in statistical physics. It was named after the physicist Ernst Ising.

Let $V = \{1, ..., n\}$ and let $\mathcal{P}_2(V)$ denote the unordered subsets of V of size 2 (assuming that $n \geq 2$). For $E \subseteq \mathcal{P}_2(V)$, an undirected graph is denoted by $G = (V, E)$ where V is the set of vertices/nodes and E is the set of edges of G. We associate to each node $i \in V$ the Bernoulli random variable I_i. Components I_i and I_j of the full random vector $\mathbf{I}$ interact "directly" only if i and j are joined by an edge in the graph.

In the context of statistical physics, these values might represent the orientations of magnets in a field, or the presence/absence of particles in a gas. In the context of image processing, these values might represent the pixel values in a black-and-white image. And in the context of social network analysis and political statistics, these values might also represent the voting patterns of politicians.

The distribution of vector $\mathbf{I}$ of the Ising model is defined for an undirected graph $G = (V, E)$ and is characterized by the following exponential family

$$p_{\mathbf{I}}(\mathbf{x}) = \exp\left(\sum_{i\in V} \theta_{ii} x_i + \sum_{(i,j)\in E} \theta_{ij} x_i x_j - A(\theta)\right) \tag{3.1}$$

where $\mathbf{x} \in \{0, 1\}^n$, $\theta = (\theta_{ij})_{i\in V,(i,j)\in E}$, and the function A satisfies

$$A(\theta) = \log \sum_{\mathbf{x}\in\{0,1\}^n} \exp\left(\sum_{i\in V} \theta_i x_i + \sum_{(i,j)\in E} \theta_{ij} x_i x_j\right).$$

Here $\theta_{ij} \in \mathbb{R}$ is the strength of edge (i, j), and $\theta_{ii} \in \mathbb{R}$ is a "potential" for node i, which models an "external field" in statistical physics, or a noisy observation in spatial statistics. For $(i, j) \notin E$, $i \neq j$, we have $I_i \perp I_j | \mathbf{I}_{\setminus\{i,j\}}$, i.e., I_i and I_j are independent given all other I's. The Ising model is said to satisfy the Pairwise Markov property.

The Ising model can be generalized in a number of different ways. Equation (3.1) includes only pairwise interactions, but it is possible to take into account higher-order interactions among the random variables. For example, to include coupling of order 3, $\{i, j, k\}$, we could add a monomial of the form $x_i x_j x_k$ with corresponding canonical parameter θ_{ijk}. Note however that higher-order interactions can also be converted to pairwise ones through the introduction of additional variables and thus retain the Markovian structure of the network. See also Dai et al. (2013) for a related generalization of the Ising model.

The size-biased versions of $\mathbf{I}$ may be characterized as distributions associated to Ising models defined on subgraphs of G. For a subset $A \subset V$, the subgraph of G induced by A is defined as $G_A := (A, E_A)$ with $E_A := \{(i, j) \in E | i \in A, j \in A\}$.

Proposition 3.1. *For $k \in \{1, 2, \ldots, n\}$, $\mathbf{I}^{[k]}$ is associated to the Ising model defined on the graph $G_{V\setminus\{k\}}$ with parameter $\theta^{[k]} = (\theta_{ij}^{[k]})_{i \in V\setminus\{k\}, (i,j) \in E_{V\setminus\{k\}}}$ satisfying, for $i \in V\setminus\{k\}$, $\theta_{ii}^{[k]} = \theta_{ii} + \theta_{ik}\mathrm{I}[(i, k) \in E]$, and, for $(i, j) \in E_{V\setminus\{k\}}$, $\theta_{ij}^{[k]} = \theta_{ij}$.*

Proof. $\mathbf{I}^{[k]}$ has for probability mass function

$$\begin{aligned} p_{\mathbf{I}^{[k]}}(\mathbf{x}) &= \frac{1}{\mathrm{E}[I_k]} p_{\mathbf{I}}(x_1, \ldots, x_{k-1}, 1, x_{k+1}, \ldots, x_n) \\ &= p_{\mathbf{I}}(\mathbf{x} | I_k = 1) \\ &= \exp\left(\sum_{i \in V\setminus\{k\}} \theta_{ii}^{[k]} x_i + \sum_{(i,j) \in E_{V\setminus\{k\}}} \theta_{ij}^{[k]} x_i x_j - A^{[k]}(\theta^{[k]}) \right). \end{aligned}$$

□

4 Decomposable graphical models

Let $G = (V, E)$ be an undirected graph. We associate to the nodes of G a random vector of claim amounts, $\mathbf{Z} = (Z_1, ..., Z_n)$, with probability density function $f_{\mathbf{Z}}$. To define decomposable graphical models for $\mathbf{Z}$, we need to introduce a few key definitions and notations.

Definition 4.1. *(Clique). A graph $G = (V, E)$ is said to be complete if $E = \mathcal{P}_2(V)$. If G_A is complete for $A \subseteq V$, A is said to be a clique of G. A maximal clique of G is a clique for which every superset of vertices of G is not a clique.*

Definition 4.2. *(Path). Let α, β be two distinct nodes in V. A path from α to β is a sequence $\alpha = \gamma_0, ..., \gamma_m = \beta$, $m \geq 1$, of distinct nodes such that, for all $1 \leq i \leq m$, $\{\gamma_{i-1,}\gamma_i\} \in E$. A cycle is a path from a node to itself.*

Definition 4.3. *(Separation). Let A, B, C be subsets of V. C is said to separate A from B if any path from $\alpha \in A$ to $\beta \in B$ intersects C.*

Definition 4.4. *(Decomposition). A pair (A, B) of subsets of V is said to be a decomposition of G if $V = A \cup B$, the subgraph induced by G on $A \cap B$ is complete and $A \cap B$ separates A from B. . If A and B are both proper subsets of V (i.e. they are strictly included in V), the decomposition is said to be proper. A graph G is said to be decomposable if it is either complete or if there exists a proper decomposition of G into two decomposable subgraphs.*

You can note that the definition of a decomposable graph is recursive. The equivalent notion of chordality may be easier to handle since a graph G is a decomposable graph if and only if G is a chordal graph (see e.g. Proposition 2.5 in Lauritzen (1996)).

Definition 4.5. *(Chordal graphs). A graph G is chordal if all cycles of four or more vertices have a chord, which is an edge that is not part of the cycle but connects two vertices of the cycle.*

Definition 4.6. *A subset S of V is a separator in G when $G_{V \setminus S}$ has more than one connected component. S is a minimal separator, when it does not contain another separator as a proper subset.*

Whenever a graph G is decomposable, the set $\mathcal{S}$ of its minimal separators can be built by the following algorithm. Begin with the empty set $\mathcal{S} = \varnothing$. Then consider a proper decomposition (A, B) of G such that $A \cap B$ is of minimal cardinality. If there is no such decomposition, it means that G is complete and stop. Otherwise, add $A \cap B$ to $\mathcal{S}$ and apply the same procedure to the subgraphs G_A and G_B. For any subset $S \in \mathcal{S}$, let $\nu(S)$ denote the number of times it appeared in the procedure. An other product of this algorithm is the set $\mathcal{C}$ containing the maximal cliques of G.

This algorithm is referred to as the junction tree algorithm because the result of this algorithm can be represented by a factor graph, i.e. a bipartite graph whose vertices are indexed by $\mathcal{C}$ and $\mathcal{S}$. Put an edge between $C \in \mathcal{C}$ and $S \in \mathcal{S}$ if and only if $C \cap S = S$. The graph obtained this way is the junction tree (see an example in Figure 1).

Whenever G is decomposable, the junction tree algorithm can be used to obtain an explicit formula for the density function of $\mathbf{Z}$ since it factorizes over G using marginal distributions over complete subsets. Indeed, if $f_{\mathbf{Z}_C}(\mathbf{z}_C)$ denotes the density function of $\mathbf{Z}_C = (Z_i)_{i \in C}$, and if $\mathcal{S}$ and $\mathcal{C}$ respectively denote the set of minimal separators and maximal cliques of G yielded by the junction tree algorithm, it can be shown that

$$f_{\mathbf{Z}}(\mathbf{z}) = \frac{\prod_{C \in \mathcal{C}} f_{\mathbf{Z}_C}(\mathbf{z}_C)}{\prod_{S \in \mathcal{S}} f_{\mathbf{Z}_S}(\mathbf{z}_S)^{\nu(S)}}. \tag{4.1}$$

(see e.g. Theorem 4 in Bartlett (2003)). Note that $\nu(S)$ is also equal to $d(S) - 1$ where $d(S)$ denotes the degree of the node corresponding to S in the junction tree (i.e. the number of edges connected to this node).

The size-biased versions of $\mathbf{Z}$ may be characterized by the same decomposable graph G (and hence with the same set of minimal separators and maximal cliques, $\mathcal{S}$ and $\mathcal{C}$). For $k \in \{1, 2, \ldots, n\}$, let $\mathcal{C}^{[k]}$ be the subset of $\mathcal{C}$ for which node $k \in C$, and $\mathcal{S}^{[k]}$ be the subset of $\mathcal{S}$ for which node $k \in C$.

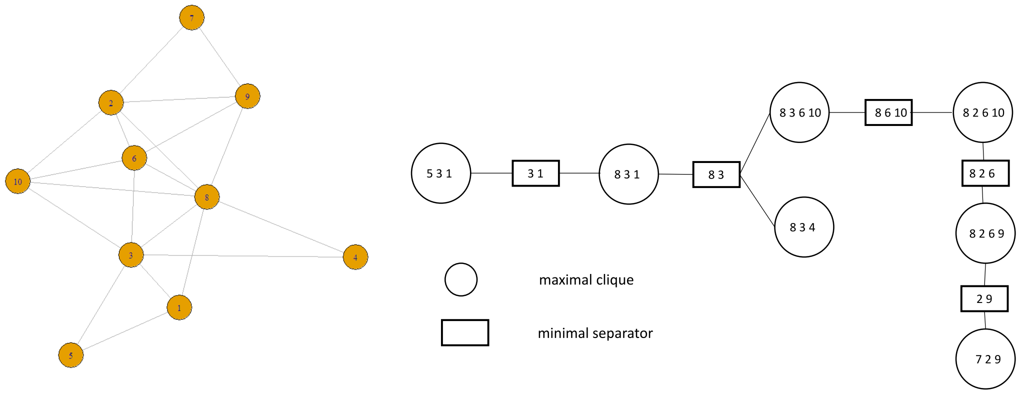

Figure 1: An example of decomposable graph with its junction tree.

Proposition 4.7. *For $k \in \{1, 2, \ldots, n\}$, $\mathbf{Z}^{[k]}$ has the following density function*

$$f_{\mathbf{Z}^{[k]}}(\mathbf{z}) = \frac{\prod_{C \in \mathcal{C}^{[k]}} f_{\mathbf{Z}_C^{[k]}}(\mathbf{z}_C)}{\prod_{S \in \mathcal{S}^{[k]}} f_{\mathbf{Z}_S^{[k]}}(\mathbf{z}_S)^{\nu(S)}} \frac{\prod_{C \in \mathcal{C} \setminus \mathcal{C}^{[k]}} f_{\mathbf{Z}_C}(\mathbf{z}_C)}{\prod_{S \in \mathcal{S} \setminus \mathcal{S}^{[k]}} f_{\mathbf{Z}_S}(\mathbf{z}_S)^{\nu(S)}}.$$

Proof. $\mathbf{Z}^{[k]}$ has for density function

$$f_{\mathbf{Z}^{[k]}}(z_1, \ldots, z_n) = \frac{z_k f_{\mathbf{Z}}(z_1, \ldots, z_n)}{\mathrm{E}[Z_k]}.$$

In the factored form of $f_{\mathbf{Z}}$ (Eq. (4.1)), z_k only appears in $f_{\mathbf{Z}_C}$ for $C \in \mathcal{C}^{[k]}$ and in $f_{\mathbf{Z}_S}$ for $S \in \mathcal{S}^{[k]}$. The result then follows by noting that

$$\frac{z_k}{\mathrm{E}[Z_k]} \frac{\prod_{C \in \mathcal{C}^{[k]}} f_{\mathbf{Z}_C}(\mathbf{z}_C)}{\prod_{S \in \mathcal{S}^{[k]}} f_{\mathbf{Z}_S}(\mathbf{z}_S)^{\nu(S)}} = \frac{\prod_{C \in \mathcal{C}^{[k]}} \left(f_{\mathbf{Z}_C}(\mathbf{z}_C) z_k / \mathrm{E}[Z_k]\right)}{\prod_{S \in \mathcal{S}^{[k]}} \left(f_{\mathbf{Z}_S}(\mathbf{z}_S) z_k / \mathrm{E}[Z_k]\right)^{\nu(S)}} = \frac{\prod_{C \in \mathcal{C}^{[k]}} f_{\mathbf{Z}_C^{[k]}}(\mathbf{z}_C)}{\prod_{S \in \mathcal{S}^{[k]}} f_{\mathbf{Z}_S^{[k]}}(\mathbf{z}_S)^{\nu(S)}}.$$

□

5 Numerical illustrations

In order to demonstrate the usefulness of the graphical model approach presented in this paper, we consider a numerical example for which the pool is composed of $n = 9$ participants. We use several R packages to generate graphs and simulate occurence and claim data:

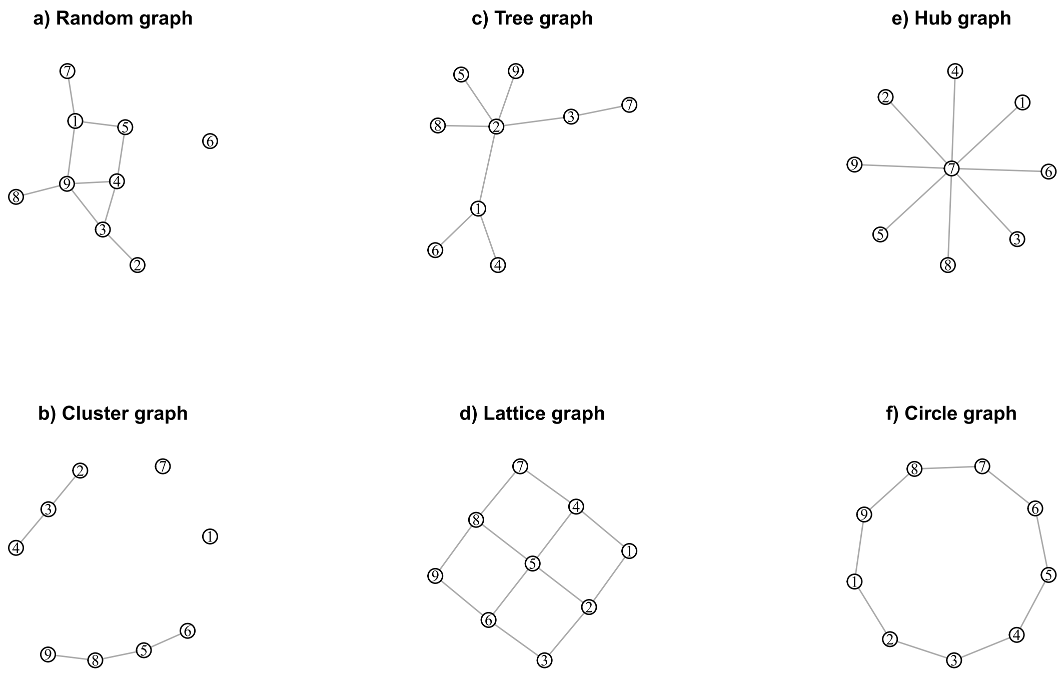

Figure 2: Ising graphs.

BDgraph for simulating multivariate distributions with different types of underlying graph structures, GLSE for generating decomposable graphs based on given numbers of vertices and edges in graphs and igraph for creating graphs from adjacency matrices.

The claim occurrences of these participants will be represented by several Ising models associated to six graphs (depicted in Figure 2): i) a random graph (edges have been chosen randomly), ii) a tree graph (edges have been chosen randomly but there is no cycle in the graph), iii) a hub graph (a non random star-shaped graph), iv) a cluster graph, v) a lattice graph (nodes are on a lattice), vi) a circle graph (nodes are on a circle). With such choices of graphs we show that it is possible to choose a graph structure suited to any practical problem.

The values of the probabilities of the Bernoulli distributions are given in Figure 3 for each graph. For the random graph, the tree graph, the hub graph and the lattice graph, these probabilities are roughly homogeneous between participants. For the cluster graph and the circle graph, one or two participants may have a probability of occurrence significantly lower than for the other participants.

We also provide in Figure 4 graphical representations of the correlation matrices of the Bernoulli vector for each graph to visualize the intensity of dependencies between occurrences of participants.

Note that the correlation coefficients may be either positive, negative or null, showing the adaptability of the Ising model. However they are bounded by functions of the probabilities

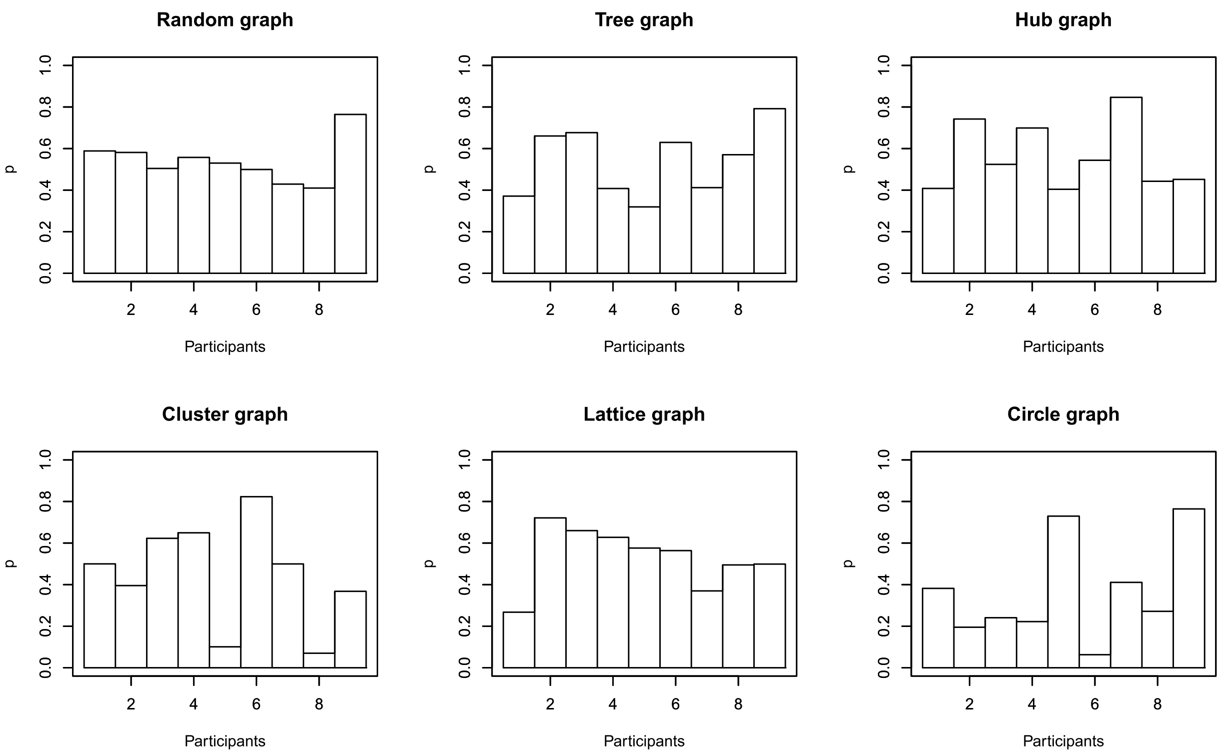

Figure 3: Ising probabilities.

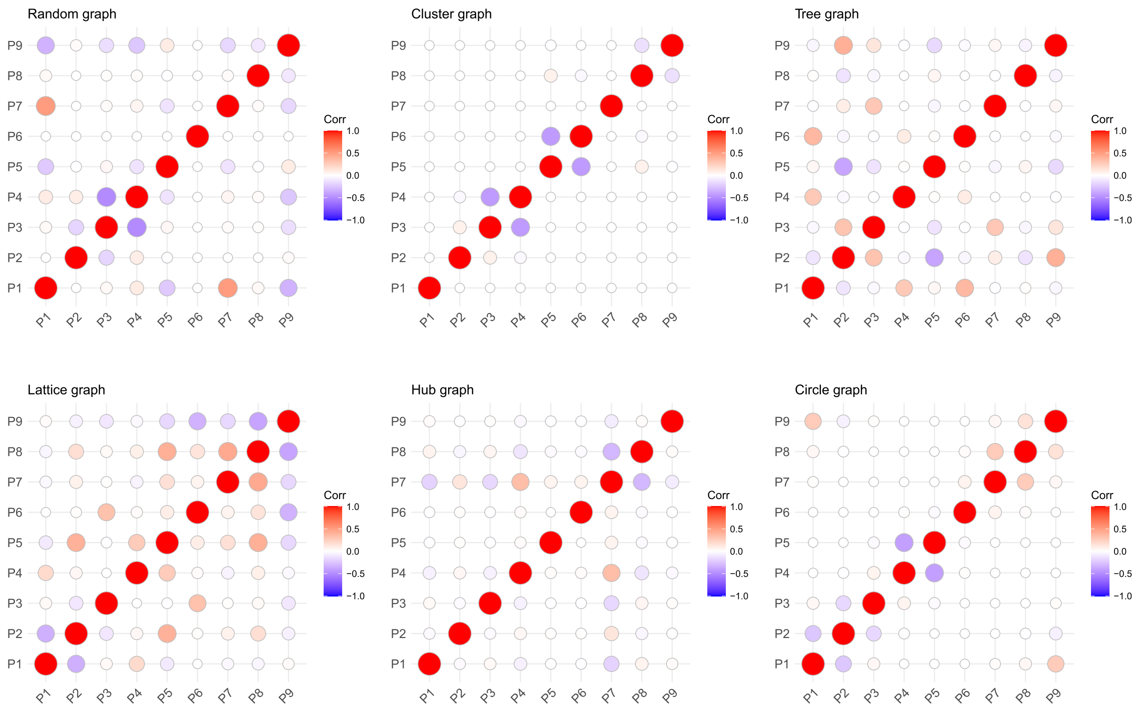

Figure 4: Correlation matrices for the Ising models.

of the (univariate) Bernoulli distributions: if ρ_{ij} denotes the correlation coefficient between I_i and I_j, then

$$\max\left(-\sqrt{\frac{p_i p_j}{(1-p_i)(1-p_j)}}, -\sqrt{\frac{(1-p_i)(1-p_j)}{p_i p_j}}\right) \leq \rho_{ij} \leq \sqrt{\frac{p_i \wedge p_j\,(1-p_i \vee p_j)}{p_i \vee p_j\,(1-p_i \wedge p_j)}},$$

as explained e.g. in p.210 of Joe (1997).

For the participants' networks, we have considered the decomposable graphs given in Figure 5. The numbers of vertices, the numbers of edges, the sets of maximal cliques and the sets of minimal seperators for all participants are given in Appendix. We selected different shapes and intensities of interconnectedness, once again to show the flexibility of the approach provided by the family of decomposable graphs.

For each participant, we chose for the distribution of his vector $\mathbf{Z}_i$ a multivariate log-normal distribution based on his decomposable graph. The means of the associated multivariate normal distributions are assumed to be equal to zero and their precision matrices (the inverse of the variance matrices) are provided in Appendix. You could note that every multivariate normal distributions defined on a maximal clique have precision matrices with non-zero entries. We finally provide on Figure 6 the histograms of the total losses for each participant. They have been obtained with 10^6 simulations. As aggregations of dependent log-normal distributions, their shape are also close from the one of a log-normal distribution. The distributions of participants 1, 2, 5, 6 and 7 appear as skewer than for the other participants.

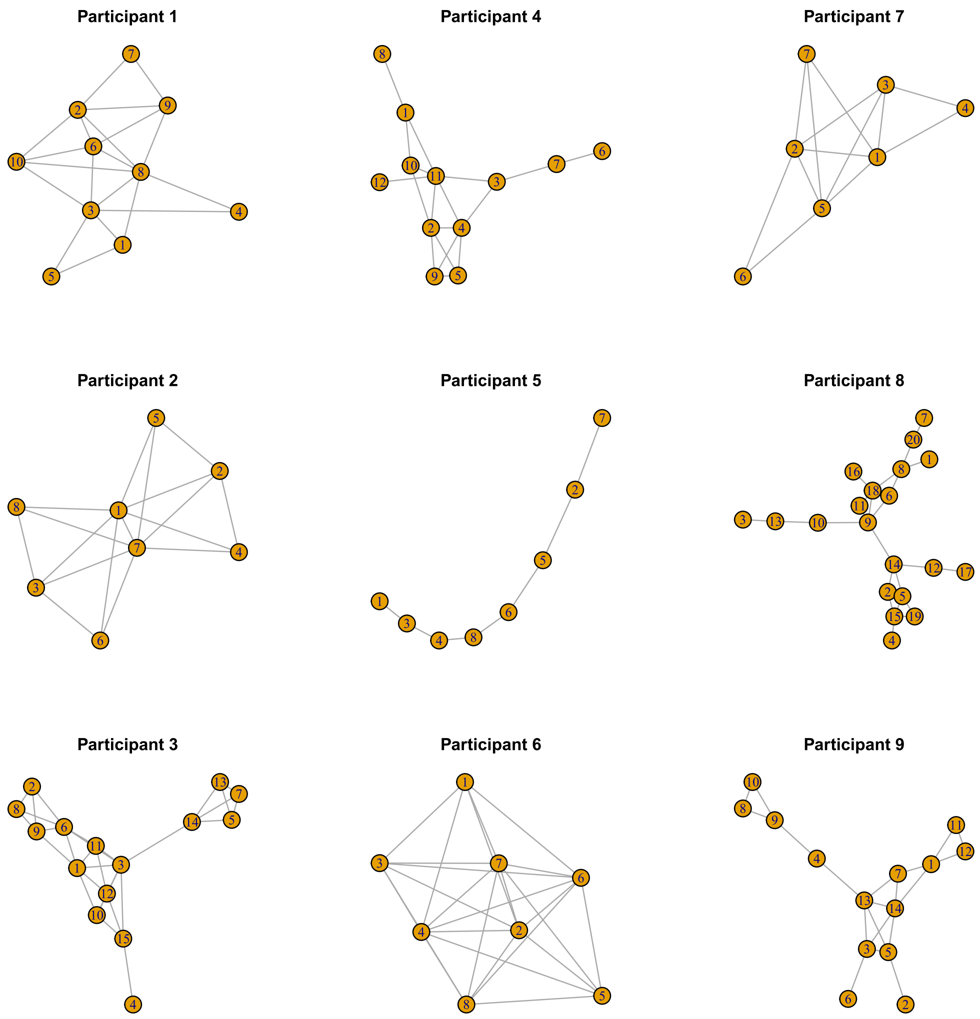

Figure 5: Participants' networks.

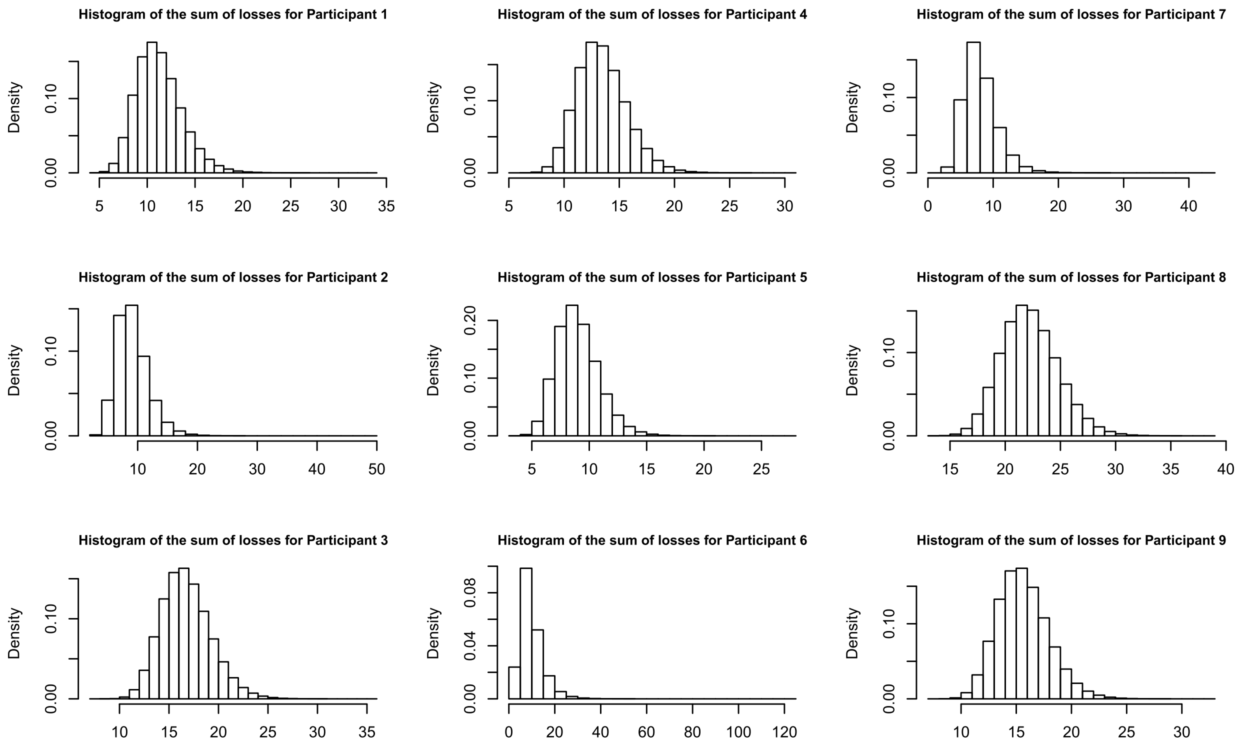

Figure 6: Histograms of participants' total losses.

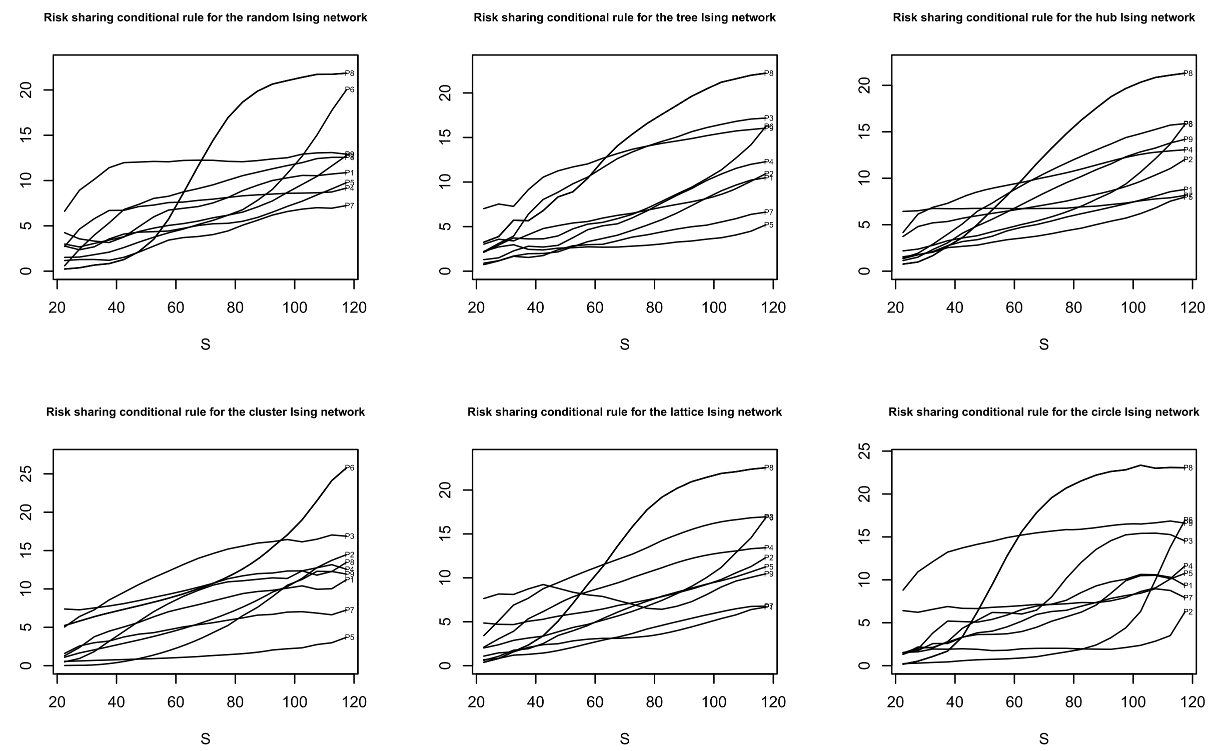

Figure 7: Conditional mean risk sharing values.

The conditional mean risk sharing values as well as the conditional mean risk sharing proportions are provided respectively in Figures 7 and 8 according to the values of the sum of the risks, S. These values have been estimated using 10^6 simulations. Depending on the Ising models, the shapes and the levels of the conditional mean risk sharing values and proportions change significantly. For example, participant 8 has the largest conditional mean risk sharing values for large S for all Ising models except for the cluster model mainly because his probability of occurence is significantly lower for this model. We can see that the curves of the conditional expectations are nonlinear most of the time (contrary to the Liouville distribution as explained in Denuit and Robert (2020d)). Note also that some curves are not increasing everywhere (e.g. participant 1 for the random Ising model or participant 9 for the lattice Ising model).

6 Conclusion and discussion

The conditional mean risk sharing rule proposed by Denuit and Dhaene (2012) has proven to be relevant for actuarial applications when risks are assumed to be independent. Denuit and Robert (2020d) provide new results for conditional expectations when risks are no more independent, but their analytical expressions may be difficult to be handled when the number of participants is large. Graphical models offer an incredible opportunity to summarize efficiently through graph-based representations of their conditional dependence structures. The

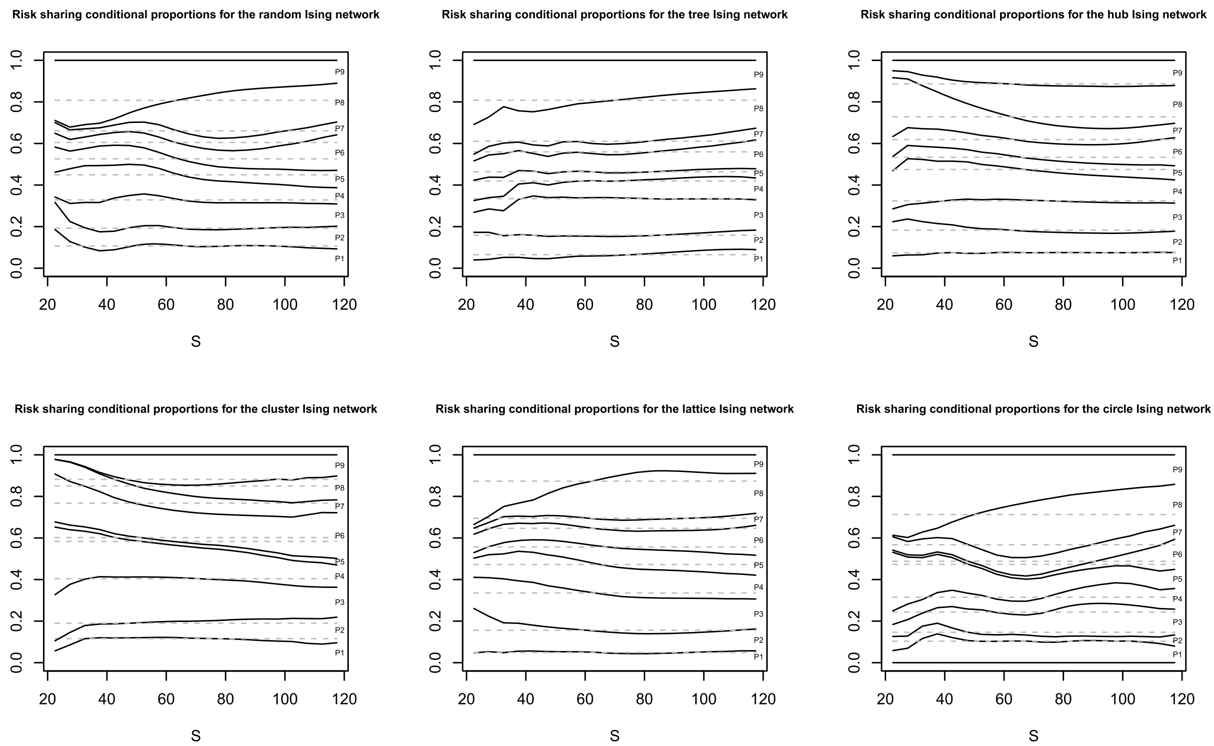

Figure 8: Cumulated conditional mean risk sharing proportions. Dashed lines provide the values of the cumulated (unconditional) mean risk sharing proportions.

Ising model for the joint occurrences of claims as well as the decomposable graphical models for claim amounts have size-biased versions that can be characterized from the same graphs or from subgraphs ot these models. Such graphical models are therefore very appealing to be used to compute the conditional mean risk sharing values.

The present paper offers practitioners new tools for managing new community-based insurance schemes when dependencies between participants or dependencies between individual claims brought by each participant can not be ignored.

References

- Arratia, R., Goldstein, L., Kochman, F. (2019). Size bias for one and all. Probability Surveys 16, 1-61.

- Bartlett, P. (2003). Undirected graphical models: chordal graphs, decomposable graphs, junction trees, and factorizations. Lecture notes.

- Dai, B., Ding, S., Wahba, G. (2013). Multivariate Bernoulli distribution. Bernoulli, 19, 4, 1465-1483.

- Denuit, M. (2019). Size-biased transform and conditional mean risk sharing, with application to P2P insurance and tontines. ASTIN Bulletin 49, 591-617.

- Denuit, M. (2020a). Size-biased risk measures of compound sums. North American Actuarial Journal, in press.

- Denuit, M. (2020b). Investing in your own and peers' risks: The simple analytics of P2P insurance. European Actuarial Journal, in press.

- Denuit, M., Dhaene, J. (2012). Convex order and comonotonic conditional mean risk sharing. Insurance: Mathematics and Economics 51, 265-270.

- Denuit, M., Robert, C.Y. (2020a). Large-loss behavior of conditional mean risk sharing. To appear in ASTIN bulletin.

- Denuit, M., Robert, C.Y. (2020b). From risk sharing to pure premium for a large number of heterogeneous losses. Submitted for publication.

- Denuit, M., Robert, C.Y. (2020c). Efron's asymptotic monotonicity property in the Gaussian stable domain of attraction. Submitted for publication.

- Denuit, M., Robert, C.Y. (2020d). Conditional tail expectation decomposition and conditional mean risk sharing for dependent and conditionally independent risks. Submitted for publication.

- Jain, K., Nanda, A.K. (1995). On multivariate weighted distributions. Communications in Statistics-Theory and Methods 24, 2517-2539.

- Joe, H. (1997). Multivariate Models and Multivariate Dependence Concepts. CRC Press.

- Lauritzen, S. (1996). Graphical Models. Oxford University.

- Lin, P., Neil, M., Fenton, N. (2014). Risk aggregation in the presence of discrete causally connected random variables. Annals of Actuarial Science, 8(02), 298-319.

- Navarro, J., Ruiz, J.M., Del Aguila, Y. (2006). Multivariate weighted distributions: A review and some extensions. Statistics 40, 51-64.

- Oberoi, J.S., Pittea, A., Tapadar, P. (2020). A graphical model approach to simulating economic variables over long horizons. Annals of Actuarial Science, 14(1), 20-41.

- Politou, D., Giudici, P. (2009). Modelling operational risk losses with graphical models and copula functions. Methodology and Computing in Applied Probability 11, 65–93.

- Ramsahai, R. (2020). Connecting actuarial judgment to probabilistic learning techniques with graph theory. arXiv:2007.15475v1.

- Xie, P., Li, J., Ou, X., Liu, P., Levy, R. (2010). Using Bayesian networks for cyber security analysis. 2010 IEEE/IFIP International Conference on Dependable Systems & Networks (DSN).

7 Appendix

Participant 1's decomposable graph and precison matrix

- Number of vertices: 10
- Number of edges: 20
- Maximal cliques

  - 1: 5 3 1 - 2: 8 3 1 - 3: 8 3 4 - 4: 8 3 6 10 - 5: 8 2 6 10 - 6: 8 2 6 9 - 7: 7 2 9
- Minimal separators

  - 1: - 2: 3 1 - 3: 8 3 - 4: 8 3 - 5: 8 6 10 - 6: 8 2 6 - 7: 2 9
- Precision matrix of the Gaussian vector:

	1	2	3	4	5	6	7	8	9	10
1	4.51	0	-0.49	0	-0.49	0	0	-0.49	0	0
2	0	4.51	0	0	0	-0.49	-0.49	-0.49	-0.49	-0.49
3	-0.49	0	4.51	-0.49	-0.49	-0.49	0	-0.49	0	-0.49
4	0	0	-0.49	4.51	0	0	0	-0.49	0	0
5	-0.49	0	-0.49	0	4.51	0	0	0	0	0
6	0	-0.49	-0.49	0	0	4.51	0	-0.49	-0.49	-0.49
7	0	-0.49	0	0	0	0	4.51	0	-0.49	0
8	-0.49	-0.49	-0.49	-0.49	0	-0.49	0	4.51	-0.49	-0.49
9	0	-0.49	0	0	0	-0.49	-0.49	-0.49	4.51	0
10	0	-0.49	-0.49	0	0	-0.49	0	-0.49	0	4.51

Participant 2's decomposable graph and precison matrix

- Number of vertices: 8
- Number of edges: 17
- Maximal cliques

  - 1: 1 7 4 2 - 2: 1 7 5 2 - 3: 1 7 3 6 - 4: 1 7 3 8
- Minimal separators

  - 1: - 2: 1 7 2 - 3: 1 7 - 4: 1 7 3
- Precision matrix of the Gaussian vector:

	1	2	3	4	5	6	7	8
1	4.39	-0.61	-0.61	-0.61	-0.61	-0.61	-0.61	-0.61
2	-0.61	4.39	0	-0.61	-0.61	0	-0.61	0
3	-0.61	0	4.39	0	0	-0.61	-0.61	-0.61
4	-0.61	-0.61	0	4.39	0	0	-0.61	0
5	-0.61	-0.61	0	0	4.39	0	-0.61	0
6	-0.61	0	-0.61	0	0	4.39	-0.61	0
7	-0.61	-0.61	-0.61	-0.61	-0.61	-0.61	4.39	-0.61
8	-0.61	0	-0.61	0	0	0	-0.61	4.39

Participant 3's decomposable graph and precison matrix

- Number of vertices: 15
- Number of edges: 30
- Maximal cliques

  - 1: 3 1 11 6 - 2: 3 1 11 12 - 3: 3 1 10 12 - 4: 3 15 12 10 - 5: 9 6 1 - 6: 2 6 8 9 - 7: 4 15 - 8: 3 14 - 9: 5 7 13 14
- Minimal separators

  - 1: - 2: 3 1 11 - 3: 3 1 12 - 4: 3 12 10 - 5: 6 1 - 6: 6 9 - 7: 15 - 8: 3 - 9: 14
- Precision matrix of the Gaussian vector:

	1	2	3	4	5	6	7	8	9	10	11	12	13	14	15
1	4.67	0	-0.33	0	0	-0.33	0	0	-0.33	-0.33	-0.33	-0.33	0	0	0
2	0	4.67	0	0	0	-0.33	0	-0.33	-0.33	0	0	0	0	0	0
3	-0.33	0	4.67	0	0	-0.33	0	0	0	-0.33	-0.33	-0.33	0	-0.33	-0.33
4	0	0	0	4.67	0	0	0	0	0	0	0	0	0	0	-0.33
5	0	0	0	0	4.67	0	-0.33	0	0	0	0	0	-0.33	-0.33	0
6	-0.33	-0.33	-0.33	0	0	4.67	0	-0.33	-0.33	0	-0.33	0	0	0	0
7	0	0	0	0	-0.33	0	4.67	0	0	0	0	0	-0.33	-0.33	0
8	0	-0.33	0	0	0	-0.33	0	4.67	-0.33	0	0	0	0	0	0
9	-0.33	-0.33	0	0	0	-0.33	0	-0.33	4.67	0	0	0	0	0	0
10	-0.33	0	-0.33	0	0	0	0	0	0	4.67	0	-0.33	0	0	-0.33
11	-0.33	0	-0.33	0	0	-0.33	0	0	0	0	4.67	-0.33	0	0	0
12	-0.33	0	-0.33	0	0	0	0	0	0	-0.33	-0.33	4.67	0	0	-0.33
13	0	0	0	0	-0.33	0	-0.33	0	0	0	0	0	4.67	-0.33	0
14	0	0	-0.33	0	-0.33	0	-0.33	0	0	0	0	0	-0.33	4.67	0
15	0	0	-0.33	-0.33	0	0	0	0	0	-0.33	0	-0.33	0	0	4.67

Participant 4's decomposable graph and precison matrix

- Number of vertices: 12
- Number of edges: 18
- Maximal cliques

  - 1: 8 1 - 2: 11 1 10 - 3: 11 2 10 - 4: 11 2 4 - 5: 11 3 4 - 6: 5 4 2 9 - 7: 7 3 - 8: 6 7 - 9: 11 12
- Minimal separators

  - 1: - 2: 1 - 3: 11 10 - 4: 11 2 - 5: 11 4 - 6: 4 2 - 7: 3 - 8: 7 - 9: 11
- Precision matrix of the Gaussian vector:

Participant 5's decomposable graph and precison matrix

- Number of vertices: 8
- Number of edges: 7
- Maximal cliques

  - 1: 1 3 - 2: 3 4 - 3: 4 8 - 4: 6 8 - 5: 6 5 - 6: 2 5 - 7: 2 7
- Minimal separators

  - 1: - 2: 3 - 3: 4 - 4: 8 - 5: 6 - 6: 5 - 7: 2
- Precision matrix of the Gaussian vector:

	1	2	3	4	5	6	7	8	9	10	11	12
1	4.59	0	0	0	0	0	0	-0.41	0	-0.41	-0.41	0
2	0	4.59	0	-0.41	-0.41	0	0	0	-0.41	-0.41	-0.41	0
3	0	0	4.59	-0.41	0	0	-0.41	0	0	0	-0.41	0
4	0	-0.41	-0.41	4.59	-0.41	0	0	0	-0.41	0	-0.41	0
5	0	-0.41	0	-0.41	4.59	0	0	0	-0.41	0	0	0
6	0	0	0	0	0	4.59	-0.41	0	0	0	0	0
7	0	0	-0.41	0	0	-0.41	4.59	0	0	0	0	0
8	-0.41	0	0	0	0	0	0	4.59	0	0	0	0
9	0	-0.41	0	-0.41	-0.41	0	0	0	4.59	0	0	0
10	-0.41	-0.41	0	0	0	0	0	0	0	4.59	-0.41	0
11	-0.41	-0.41	-0.41	-0.41	0	0	0	0	0	-0.41	4.59	-0.41
12	0	0	0	0	0	0	0	0	0	0	-0.41	4.59

	1	2	3	4	5	6	7	8
1	4.39	0	-0.61	0	0	0	0	0
2	0	4.39	0	0	-0.61	0	-0.61	0
3	-0.61	0	4.39	-0.61	0	0	0	0
4	0	0	-0.61	4.39	0	0	0	-0.61
5	0	-0.61	0	0	4.39	-0.61	0	0
6	0	0	0	0	-0.61	4.39	0	-0.61
7	0	-0.61	0	0	0	0	4.39	0
8	0	0	0	-0.61	0	-0.61	0	4.39

Participant 6's decomposable graph and precison matrix

- Number of vertices: 8
- Number of edges: 25
- Maximal cliques
  - 1: 2 4 6 7 3 1 - 2: 2 4 6 7 3 8 - 3: 2 4 6 7 5 8
- Minimal separators
  - 1: - 2: 2 4 6 7 3 - 3: 2 4 6 7 8
- Precision matrix of the Gaussian vector:

	1	2	3	4	5	6	7	8
1	4.39	-0.61	-0.61	-0.61	0	-0.61	-0.61	0
2	-0.61	4.39	-0.61	-0.61	-0.61	-0.61	-0.61	-0.61
3	-0.61	-0.61	4.39	-0.61	0	-0.61	-0.61	-0.61
4	-0.61	-0.61	-0.61	4.39	-0.61	-0.61	-0.61	-0.61
5	0	-0.61	0	-0.61	4.39	-0.61	-0.61	-0.61
6	-0.61	-0.61	-0.61	-0.61	-0.61	4.39	-0.61	-0.61
7	-0.61	-0.61	-0.61	-0.61	-0.61	-0.61	4.39	-0.61
8	0	-0.61	-0.61	-0.61	-0.61	-0.61	-0.61	4.39

Participant 7's decomposable graph and precison matrix

- Number of vertices: 7
- Number of edges: 13
- Maximal cliques

  - 1: 1 2 5 3 - 2: 1 2 5 7 - 3: 6 5 2 - 4: 1 4 3
- Minimal separators

  - 1: - 2: 1 2 5 - 3: 5 2 - 4: 1 3
- Precision matrix of the Gaussian vector:

	1	2	3	4	5	6	7
1	4.31	-0.69	-0.69	-0.69	-0.69	0	-0.69
2	-0.69	4.31	-0.69	0	-0.69	-0.69	-0.69
3	-0.69	-0.69	4.31	-0.69	-0.69	0	0
4	-0.69	0	-0.69	4.31	0	0	0
5	-0.69	-0.69	-0.69	0	4.31	-0.69	-0.69
6	0	-0.69	0	0	-0.69	4.31	0
7	-0.69	-0.69	0	0	-0.69	0	4.31

Participant 8's decomposable graph and precison matrix

- Number of vertices: 20
- Number of edges: 25
- Maximal cliques

  - 1: 8 1 - 2: 8 6 18 - 3: 9 18 6 - 4: 9 18 11 - 5: 9 10 - 6: 13 10 - 7: 3 13 - 8: 9 14 - 9: 2 5 14 - 10: 2 5 15 - 11: 5 19 15 - 12: 4 15 - 13: 16 18 - 14: 12 14 - 15: 12 17 - 16: 8 20 - 17: 7 20
- Minimal separators

  - 1: - 2: 8 - 3: 18 6 - 4: 9 18 - 5: 9 - 6: 10 - 7: 13 - 8: 9 - 9: 14 - 10: 2 5 - 11: 5 15 - 12: 15 - 13: 18 - 14: 14 - 15: 12 - 16: 8 - 17: 20
- Precision matrix of the Gaussian vector:

	1	2	3	4	5	6	7	8	9	10	11	12	13	14	15	16	17	18	19	20
1	4.75	0	0	0	0	0	0	-0.25	0	0	0	0	0	0	0	0	0	0	0	0
2	0	4.75	0	0	-0.25	0	0	0	0	0	0	0	0	-0.25	-0.25	0	0	0	0	0
3	0	0	4.75	0	0	0	0	0	0	0	0	0	-0.25	0	0	0	0	0	0	0
4	0	0	0	4.75	0	0	0	0	0	0	0	0	0	0	-0.25	0	0	0	0	0
5	0	-0.25	0	0	4.75	0	0	0	0	0	0	0	0	-0.25	-0.25	0	0	0	-0.25	0
6	0	0	0	0	0	4.75	0	-0.25	-0.25	0	0	0	0	0	0	0	0	-0.25	0	0
7	0	0	0	0	0	0	4.75	0	0	0	0	0	0	0	0	0	0	0	0	-0.25
8	-0.25	0	0	0	0	-0.25	0	4.75	0	0	0	0	0	0	0	0	0	-0.25	0	-0.25
9	0	0	0	0	0	-0.25	0	0	4.75	-0.25	-0.25	0	0	-0.25	0	0	0	-0.25	0	0
10	0	0	0	0	0	0	0	0	-0.25	4.75	0	0	-0.25	0	0	0	0	0	0	0
11	0	0	0	0	0	0	0	0	-0.25	0	4.75	0	0	0	0	0	0	-0.25	0	0
12	0	0	0	0	0	0	0	0	0	0	0	4.75	0	-0.25	0	0	-0.25	0	0	0
13	0	0	-0.25	0	0	0	0	0	0	-0.25	0	0	4.75	0	0	0	0	0	0	0
14	0	-0.25	0	0	-0.25	0	0	0	-0.25	0	0	-0.25	0	4.75	0	0	0	0	0	0
15	0	-0.25	0	-0.25	-0.25	0	0	0	0	0	0	0	0	0	4.75	0	0	0	-0.25	0
16	0	0	0	0	0	0	0	0	0	0	0	0	0	0	0	4.75	0	-0.25	0	0
17	0	0	0	0	0	0	0	0	0	0	0	-0.25	0	0	0	0	4.75	0	0	0
18	0	0	0	0	0	-0.25	0	-0.25	-0.25	0	-0.25	0	0	0	0	-0.25	0	4.75	0	0
19	0	0	0	0	-0.25	0	0	0	0	0	0	0	0	0	-0.25	0	0	0	4.75	0
20	0	0	0	0	0	0	-0.25	-0.25	0	0	0	0	0	0	0	0	0	0	0	4.75

Participant 9's decomposable graph and precison matrix

- Number of vertices: 14
- Number of edges: 20
- Maximal cliques

- 1: 1 7 14 - 2: 13 14 7 - 3: 13 14 5 3 - 4: 2 5 - 5: 13 4 - 6: 9 4 - 7: 8 9 10 - 8: 11 12 1 - 9: 6 3

- Minimal separators

- 1: - 2: 14 7 - 3: 13 14 - 4: 5 - 5: 13 - 6: 4 - 7: 9 - 8: 1 - 9: 3

- Precision matrix of the Gaussian vector:

	1	2	3	4	5	6	7	8	9	10	11	12	13	14
1	4.65	0	0	0	0	0	-0.35	0	0	0	-0.35	-0.35	0	-0.35
2	0	4.65	0	0	-0.35	0	0	0	0	0	0	0	0	0
3	0	0	4.65	0	-0.35	-0.35	0	0	0	0	0	0	-0.35	-0.35
4	0	0	0	4.65	0	0	0	0	-0.35	0	0	0	-0.35	0
5	0	-0.35	-0.35	0	4.65	0	0	0	0	0	0	0	-0.35	-0.35
6	0	0	-0.35	0	0	4.65	0	0	0	0	0	0	0	0
7	-0.35	0	0	0	0	0	4.65	0	0	0	0	0	-0.35	-0.35
8	0	0	0	0	0	0	0	4.65	-0.35	-0.35	0	0	0	0
9	0	0	0	-0.35	0	0	0	-0.35	4.65	-0.35	0	0	0	0
10	0	0	0	0	0	0	0	-0.35	-0.35	4.65	0	0	0	0
11	-0.35	0	0	0	0	0	0	0	0	0	4.65	-0.35	0	0
12	-0.35	0	0	0	0	0	0	0	0	0	-0.35	4.65	0	0
13	0	0	-0.35	-0.35	-0.35	0	-0.35	0	0	0	0	0	4.65	-0.35
14	-0.35	0	-0.35	0	-0.35	0	-0.35	0	0	0	0	0	-0.35	4.65